

## Conformable Actuation and Sensing with Robotic Fabric

Michelle Yuen<sup>1</sup>, Arun Cherian<sup>1</sup>, Jennifer C. Case<sup>1</sup>, Justin Seipel<sup>1</sup>, Rebecca K. Kramer<sup>1\*</sup>

**Abstract**—Future generations of wearable robots will include systems constructed from conformable materials that do not constrain the natural motions of the wearer. Fabrics represent a class of highly conformable materials that have the potential for embedded function and are highly integrated into our daily lives. In this work, we present a robotic fabric with embedded actuation and sensing. Attaching the same robotic fabric to a soft body in different ways leads to unique motions and sensor modalities with many different applications for robotics. In one mode, the robotic fabric acts around the circumference of the body, and compression of the body is achieved. Attaching the robotic fabric in another way, along one surface of a body for example, bending is achieved. We use thread-like actuators and sensors to functionalize fabric via a standard textile manufacturing process (sewing). The actuated fabric presented herein yields a contractile force of 9.6N and changes in length by approximately 60% when unconstrained. The integrated strain sensor is evaluated and found to have an RMS error of 14.6%, and qualitatively differentiates between the compressive and bending motions demonstrated.

### I. INTRODUCTION

Robots have the incredible power to amplify human productivity and enhance our capabilities, and by doing so shape the world we live in. The use of the word robotic implies a rigid, bulky, and complex device; however, the emerging fields of soft robotics and wearable robotics counter this implication by exploring the use of conformable materials as actuators and sensors. In particular, we believe that fabrics will play a large role in the future of soft and wearable robots, and could be employed in applications such as active clothing, active joint braces, or wearable interfaces. By treating clothing as a field of engineering, it can be transformed from passive apparel to active equipment, assisting its wearer by enhancing strength, improving stamina, or preventing injury. As fabrics are already heavily integrated into our daily lives, robotic fabrics will be natural for people to wear and interact with, both minimizing discomfort and maximizing efficiency.

Robotic fabrics can also be customizable across different hosts and utilized differently depending on the host. For example, a fabric sleeve with intermittent compression actuators may be worn by a human to create peristaltic-like flow of fluids within the muscle to aid in post-exertion recovery, and this same fabric could be placed on a cylindrical deformable body to create peristaltic-like locomotion. Similarly, a linearly actuating fabric might be applied to produce contraction, bending or compression of different hosts.

\*Author to whom correspondence should be addressed  
rebeccakramer@purdue.edu

<sup>1</sup>School of Mechanical Engineering, Purdue University, West Lafayette, IN 47907, USA

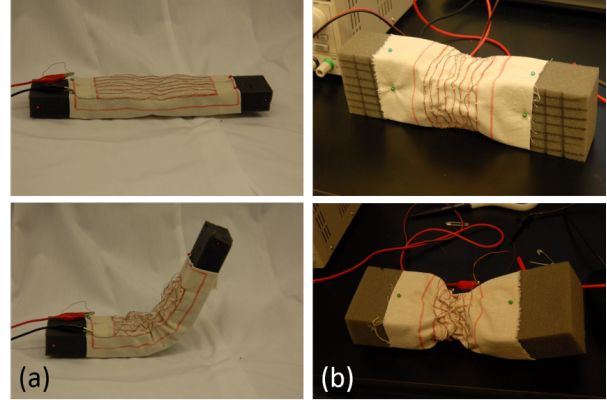


Fig. 1: Application of the same robotic fabric towards different modes of motion: (a) flexing of a hinge joint and (b) compressing a soft body.

In this work, we present a functionalized fabric embedded with actuators and sensors. Because the actuators and sensors integrated in the fabric base are also thread-like in terms of shape, size and flexibility, the functionalized fabric retains the conformable nature of its fabric base. To illustrate the versatility of robotic fabrics, we present two modes of actuation using the same robotic fabric on a soft foam block: (1) bending, employing linear contraction along the length of the foam, and (2) compression, employing radial pressure by wrapping the fabric around the foam midsection. For both modes of actuation, we test and report on the behavior of the robotic fabric.

We use shape-memory alloy (SMA) wire as the actuation mechanism. The SMA is programmed to remember a helical coil when heated, which was previously shown to increase the actuator change in length from between 4-10% to as much as 50% [1]. The sensors used in this study are custom-made by filling soft silicone tubing with liquid-metal. When the tubing is strained or compressed, the cross-sectional area of the encased liquid-metal is deformed, resulting in a change in electrical resistance. Both the actuator and sensor components were chosen to mimic the compliance, strength, and usability of threads in fabric. As such, they can be integrated with fabrics using standard textile manufacturing approaches, such as sewing.

Robotic fabrics could be incorporated into wearable interfaces and electronics such as communication devices, wire harnesses and conformable antennas, as well as assistive fabrics for motion aid, prolonged endurance, and health-monitoring. Furthermore, robotic fabrics have applications in on-the-fly robot design in cases where function may need

to be adjusted on-demand, such as with exploratory robots or first-responder robots.

## II. PREVIOUS WORK

Smart fabrics [2], [3], [4], [5] are generally fabrics that incorporate some electronic component(s) for medical monitoring or wearable computing [6], [7]. Components and connections are meant to be intrinsic to the fabric and therefore less intrusive in daily tasks than other potential forms of wearable computing. Some examples include the integration of fiber optic sensors into fabrics [8], [9], textile piezoresistive sensors [10], transistors in/on fibers [11], [12], and conductive threads [13], [14], [15], [16]. Furthermore, smart textiles may utilize mainstream textile manufacturing techniques, such as weaving [17], [18], [19] and knitting [20], which holds promise for fast integration times and process scalability.

While existing electronic fabrics have established exciting possibilities for sensing in a conformable, soft, wearable context, these do not yet have the capability of integrating both sensing and actuation. Some recent demonstrations of actuating systems that are comparable to fabrics include an active soft orthotic device [21] and a soft exosuit made from pneumatic actuators and inextensible webbing [22]. These soft exoskeleton architectures are designed to reduce impact on the wearer's normal kinematics by completely removing rigid elements. Another related example is that demonstrated by Seok, *et al.*, where peristaltic locomotion was achieved with a flexible braided mesh-tube structure with integrated NiTi coil actuators [23]. In these cases, the actuating systems have been designed for a very particular function, such as assisted joint motion on a human wearer or locomotion via compression of a deformable body. We counter this mindset by exploring the use a single actuating fabric that may be transferred between hosts with the purpose of achieving variable modes of actuation. By simply changing either the host or orientation of the fabric, a different function may be enabled.

In this paper, we demonstrate the following two innovations: (1) integrated actuation and sensing in a functional and conformable fabric, and (2) versatility in actuation mode from the same robotic fabric, which may be controlled by the position of the fabric and the deformable body it is on.

## III. FABRICATION

The robotic fabric begins with a base fabric of muslin, an inelastic woven cotton textile. Because the fabric is flexible and non-extensible, the deformation of the SMA wire is transferred more fully to the overall end-to-end displacement of the entire swatch of fabric. A stiffer fabric would resist the deformation; a more elastic fabric will have reduced end-to-end force production due to in-fabric stretching.

The actuator consists of nickel titanium (NiTi) shape memory alloy (SMA) wire. The SMA wire (Dynalloy 70°C, 0.015" dia.) is programmed by first coiling it tightly along a shaft (McMaster Carr, 0.25" dia. steel shaft) and fixing the ends using shaft collars (McMaster Carr, two-piece clamp-on

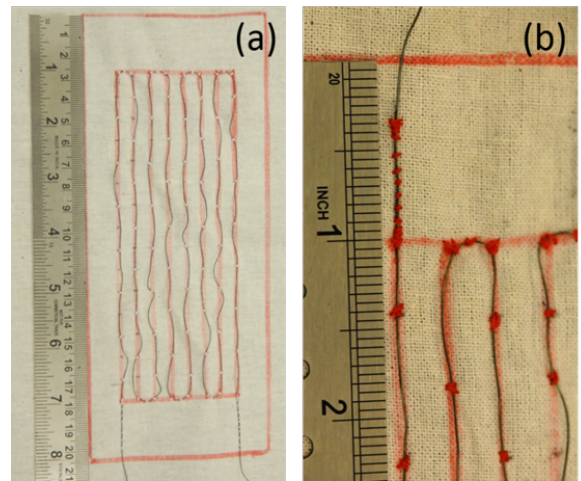


Fig. 2: (a) SMA wire stitched to fabric base. Dimensions of the wire area: 2.265" x 6". Wire spacing: 0.375". Stitch length: 0.785". (b) A closer look at the stitching of the SMA wire onto muslin.

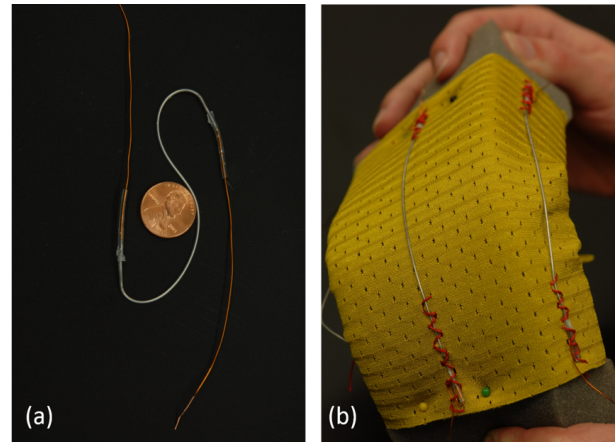


Fig. 3: (a) A sensor thread composed of eGaIn-filled hyperelastic silicone tubing. (b) Sensor threads attached to fabric via couching and wrapped around a foam block.

shaft collar for 0.25" dia. shaft) to maintain tension in the wire. The shaft and wire are then heated at 500°C for 15 minutes in a furnace (Thermo Scientific Lindberg Blue M) and quenched in cold water, over 5 intervals. The SMA wire is then unwound and sewn onto the fabric base in a serpentine pattern as seen in Figure 2. By using a serpentine pattern, the contractile force of a single SMA wire is extended across an area. The wire is laid upon the fabric in the desired pattern and then cross-stitched in place by hand with an inelastic cotton thread. Alternatively, the SMA wire can be fed through the lower bobbin in a sewing machine and lock-stitched into place. In order to maximize the end-to-end displacement of the fabric, the stitch length (i.e. the spacing between anchoring points) is equal to the circumference of the programmed helical coil. With this spacing, an entire loop is allowed to form when the SMA is heated. In contrast, if the stitches were spaced closer together, the SMA would be more restrained to the fabric and fail to regain the programmed coil as readily.

The sensors, hereby referred to as sensor threads, consist of hyperelastic tubing (High Purity White Silicone Tubing, McMaster-Carr, outer diameter 0.037") filled with eutectic gallium indium (eGaIn), a non-toxic conductive liquid alternative to mercury (Figure 3a). A length of silicone tubing is first filled with eGaIn by injecting it through the tubing with a syringe. Copper wire is inserted into the ends of the sensors to serve as lead wires. The sensors are sealed by encasing silicone caulk at the wire-tubing interface with heat shrink tubing. After allowing the caulk to cure, heat is applied to the heat-shrink tubing to complete the sealing process.

The sensor thread is secured onto the fabric base by couching the heat shrink tubing onto the fabric as shown in Figure 3b. Couching is a method of securing a yarn onto a fabric by stitching another thread around the yarn, harnessing the yarn to the fabric. Only the ends of the sensor threads covered with heat shrink tubing are couched onto the fabric to prevent the thread from compressing the silicone tubing and provoking a false report of strain. The sensors and SMA are attached on opposite sides of the fabric to reduce the possibility of damaging the tubing through heating or pinching when the SMA is activated. The sensors are pretensioned with approximately 60% strain when attaching them to the fabric base such that the sensor experiences zero strain when the robotic fabric is fully contracted. As a result, when the fabric is flat, the sensor undergoes a positive 60% strain.

Considerations of the robotic fabrics intended geometry are used to determine the placement, length and orientation of the sensor threads. For example, to measure the amount of bending in a body, sensors are laid parallel to the anticipated direction of bending as shown in Figure 3b. By reading the resistance output of multiple sensors arranged on a body, the deformation and curvature of the body can be obtained.

#### IV. CHARACTERIZATION

##### A. Actuator Characterization

In order to characterize the performance of SMA integrated in the fabric for linear isometric force generation, we fabricated a rectangular swatch with dimensions 2.625" x 6" containing 8 returns of SMA spaced 0.375" apart. The length of the swatch was maintained constant between the jaws of a materials testing machine (Instron 3345) (Figure 4). The unit was actuated by a power supply outputting a constant 10V and a maximum of 1.2A, prompting the SMA to recall its programmed shape, a helical coil of diameter 0.25". Because the length of the unit was maintained constant, an increase in force was measured.

The force was recorded over 15 cycles of powering the SMA on and off at 10V and 1.2A over 30s and 60s time intervals, respectively (Figure 5). The actuator unit was found to degrade in performance in terms of force production by 9.8% after 5 cycles and 17.4% after 15 cycles due to degradation of the shape memory effect of the SMA, as well as stretching of the base fabric and stitching thread. It is assumed that the degradation will continue due to weakening of the fabric and stitch threads. The maximum force

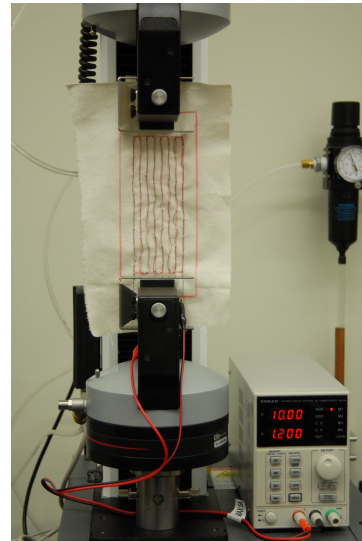


Fig. 4: Characterization of linear force generation by a single actuator unit using a materials testing machine.

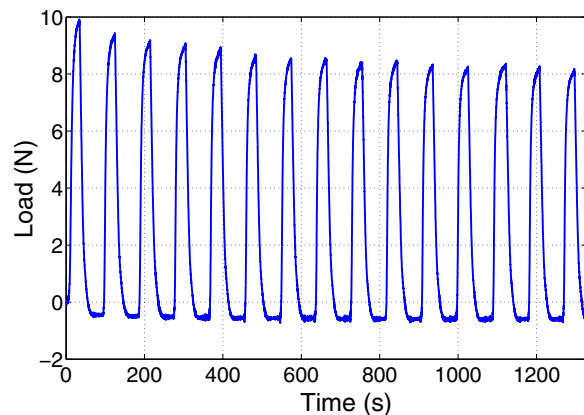


Fig. 5: Plot of the force produced by a single actuator unit in isometric contraction over 15 cycles. The fabric swatch had dimensions 2.625" x 6" and contained 8 returns of programmed SMA spaced 0.375" apart. SMA was powered at 10V and 1.2A.

generated by the actuation unit, for which the total length of SMA was 50.625", was approximately 9.6N. When allowed to freely contract, the fabric contracted approximately 60% in length. This linear force and displacement may be translated to bulk radial pressure when the fabric is wrapped around a host. While a rough estimate may be obtained by assuming that the stress in the actuator is linearly proportional to the hoop stress (as given by pressure vessel analysis), actual distributed pressure will depend largely on properties of the host such as size, shape, elasticity, and compressibility.

##### B. Sensor Characterization

To determine the sensor threads resistive response to strain, an Instron materials testing machine was used to apply strain to the device at a rate of 50mm/min from 0 to 100%. Simultaneously, a BK Precision 5492B digital multimeter recorded the resistance at a rate of 2Hz. As the sensors are stretched, the cross-section decreases and

the overall length increases. This results in an increase in resistance as  $R = \rho \frac{L}{A}$ , where  $\rho$  is the resistivity of eGaIn,  $L$  and  $A$  are the length and cross-sectional area of the sensor, respectively. The experimental data relating strain to the normalized change in resistance of the sensor ( $dR/R_0$ ) was plotted to determine the characteristic behavior of each sensor (Figure 6).

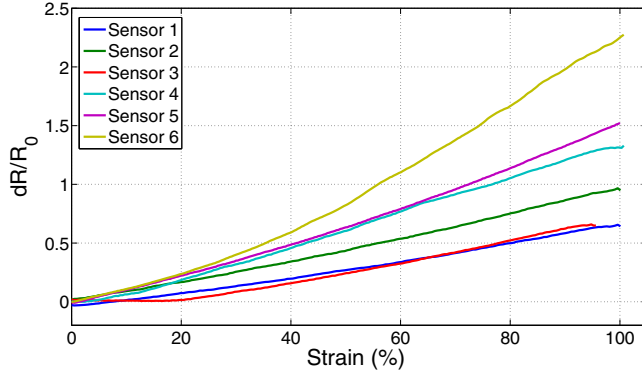


Fig. 6: Resistive response of 6 sensor threads of the same geometry to applied strain at a rate of 50mm/min. Data has been smoothed by a running average over 10 data points.

Figure 6 plots the response of 6 individual threads of the same dimensions (outer dia. 0.037", length 5"). While the strain characterization data appears to follow a 2nd-order polynomial model, within the range of 0 to 100% strain, the data can also be approximated by a linear model. Although plotted outputs are normalized by the initial resistance of each sensor by  $dR/R_0$ , the responses are clearly inconsistent across different specimens of the same design specifications. This implies imperfections in the manufacturing process (e.g. sealing, wire-eGaIn interface) that must be addressed for consistent product yield and the need for individual empirical characterization of each sensor.

## V. RESULTS

### A. Bending

Robotic fabric was pinned across a hinge joint in a foam block such that during activation, the fabric would remain secured to the surface of the foam block, thus causing the arms to bend together (Figure 7). The SMA was powered at a constant voltage of 10V and a maximum current of 1.2A for 50s, which ensured that the SMA would reach maximal force production as seen in Figure 5. The force produced was sufficient to decrease the joint angle by approximately 80°. After the power to the actuation unit was turned off, the foam body and the fabric were allowed to relax to a final state. Because the foam block did not provide sufficient rebounding force, the SMA remained in a semi-contracted state and the joint remained slightly bent.

The joint angle can be approximated from the sensory data. Because the sensor is pretensioned when attaching it to the fabric, it experiences maximal strain when the joint angle is 180°, i.e. when the fabric is flat. As the joint is flexed due to contraction of the SMA, the sensor experiences less strain.

This is demonstrated in the plot of  $dR/R_0$  in Figure 7, where the output resistance decreases as the joint angle decreases. Characterization of the sensor threads focused solely on the response due to linear strain (Figure 6). To translate linear strain to proprioceptive capability in a bending application, the joint angle can be calculated via the law of cosines as  $\theta = \arccos(\frac{a^2+b^2-L^2}{2ab})$ , where  $a$  and  $b$  are the distances between the ends of the sensor and the axis of rotation and  $L$  is the length of the sensor. Length  $L$  is calculated by applying the empirically found linear model to the normalized resistance output of the sensor due to applied strain.

To empirically verify proprioceptive capability, the output of a sensor thread was recorded at various joint angles from approximately 90° to 180°. The sensor was attached to the arms of the joint while the joint angle was 180° with a pre-strain of 60%; at 90°, the distance between the attachment points was slightly less than the initial length of the sensor. The actual joint angle was determined by measuring the angle in photos taken directly from the side during the test. The empirical calibration demonstrated a linear relationship between the joint angle and the normalized resistance, which is consistent with the linear characterization reported in Figure 6. Analysis of the calibration data yielded the regression equation:  $\theta = 108.46 \frac{dR}{R_0} + 103.61$ , which was used to calculate the expected joint angle given a normalized resistance value. A comparison of the actual and expected joint angle given a normalized resistance output is plotted in Figure 8. The RMS error between the actual and expected joint angle was found to be 14.6%. At low bend angles, the accuracy of the sensor degrades because the sensor was slack and had a near-zero normalized resistance output. Once out of this range (approximately 115-120°), the accuracy of the sensor improved due to sufficient tension across the sensor. To increase the range of angles that can be measured, more sensors can be placed around the joint and different methods of sensing can be used.

### B. Compression

The same swatch of robotic fabric was wrapped around and then pinned to a foam block with the sensor thread between the fabric and the foam (Figure 9). The SMA was activated with 10V and 1.2A for 2 minutes then deactivated; the resistance output of the sensor was continuously recorded. In contrast to the bending application, the resistance of the sensor increased as the SMA was activated. As the fabric squeezed the foam, it also applied pressure to the sensor. Because the resistance of the sensor thread is  $R = \frac{\rho L}{A}$ , the decrease in cross-sectional area,  $A$ , results in an increase in resistance,  $R$ . The effect of pressure on this device has not yet been conclusively characterized; however, previously developed elastomer-based pressure sensors operate on this basic principle [24], [25]. The resistance increased somewhat linearly up to the maximum compression, at which point the SMA was deactivated. As the SMA cooled, it maintained a semi-contracted state due to an insufficient restoring force to decompress the foam and re-extend the SMA wire.

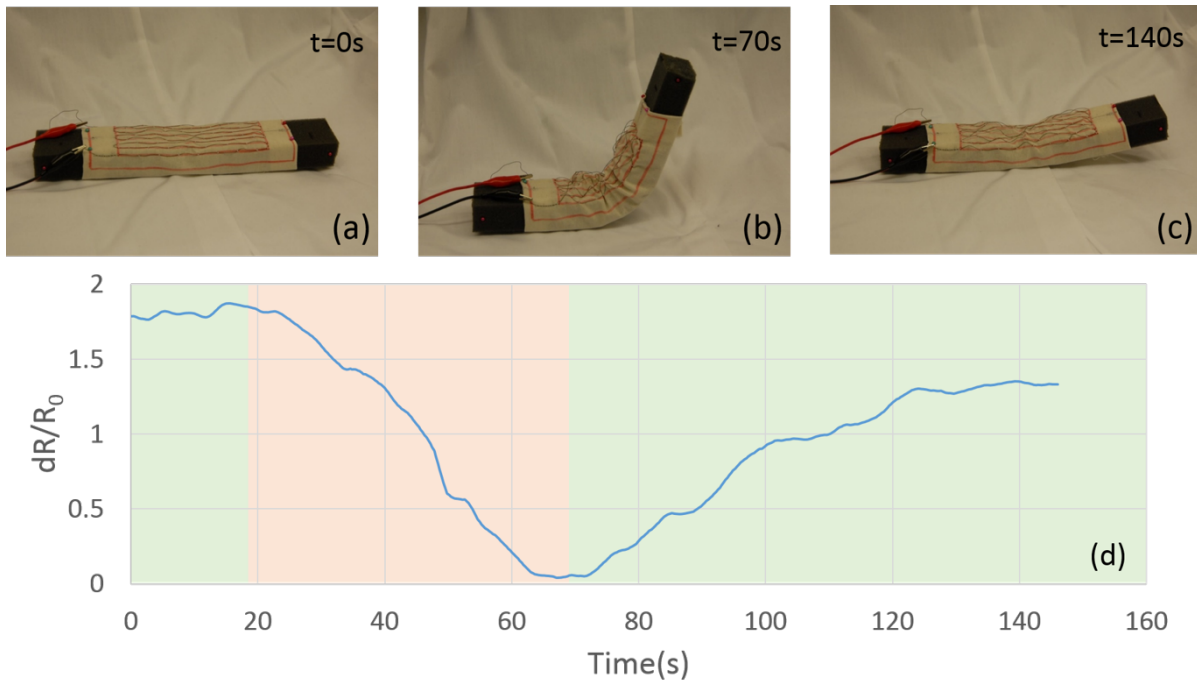


Fig. 7: (a)-(c) Photos of a bending application showing the initial state, the maximum bending position, and the final relaxed state. (d) Sensor output during flexure of a joint. The red and green shading indicate powered and unpowered SMA, respectively. Data has been smoothed by averaging over 10 data points.

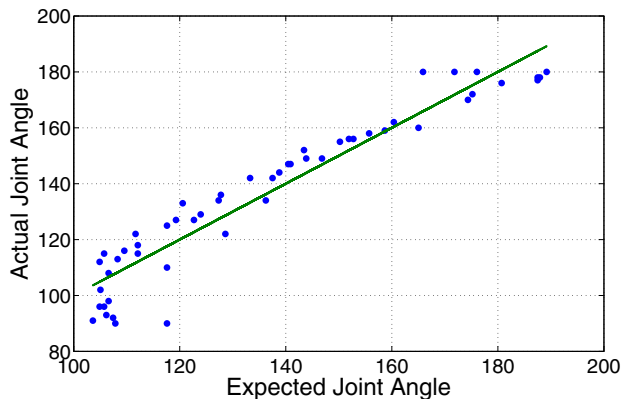


Fig. 8: Comparison of actual and expected joint angles. The expected joint angle was calculated from  $\theta = 108.46 \frac{dR}{R_0} + 103.61$  as determined during prior empirical sensor calibration.

## VI. DISCUSSION

When the robotic fabric is attached to a face of the body such that the active threads act more on one side of the body than another, bending occurs. Even if robotic fabric is attached on all sides or faces of a body and co-activation occurs, if there is net actuation to one side of the body, then bending occurs to that side. The bending motion of a soft body can also be approximated by bending beam theory, lending itself to fundamental analysis and predictive modeling.

Bending is a fundamental mode of motion with many applications for robotics. Bending is representative of motions

that are typically associated with bending of a spine or the bending of an articulated limb, and many traditional robotics applications have been developed [26], [27], [28]. Robotic fabric may have applications in traditional robotic settings, as there is a need for softer and safer robots in industry and in human environments. Soft and partially articulated bodies could bend and function effectively like an articulated limb as the robotic fabric matrix acts effectively like the antagonist pairs of muscles that occur across joints. To assist motion of a human wearer, fabric that spans articulated joints could generate additional bending moments beyond what a human achieves with his or her own muscles. Such robotic fabric spanning across a human joint would act like an additional thin layer of muscle on top of the musculoskeletal complex of the joint.

When the robotic fabric is attached to a foam block such that the active threads act around the circumference, it produces a net pressure on the surface of the body that causes a compressive deformation. The compression of a circumferential robotic fabric has immediate relevance for robotics applications ranging from wearable compression suits to soft-bodied locomotion like peristalsis (e.g. earthworm locomotion) [21], [22], [23]. To achieve a wearable and active compression garment, active threads would be oriented around the circumference of limbs and the trunk of the human body. This would enable the control of static pressure and cyclic pressure over desired portions of limbs and the trunk.

Although the current sensing capabilities of robotic fabric cannot be relied upon for their quantitative accuracy, their

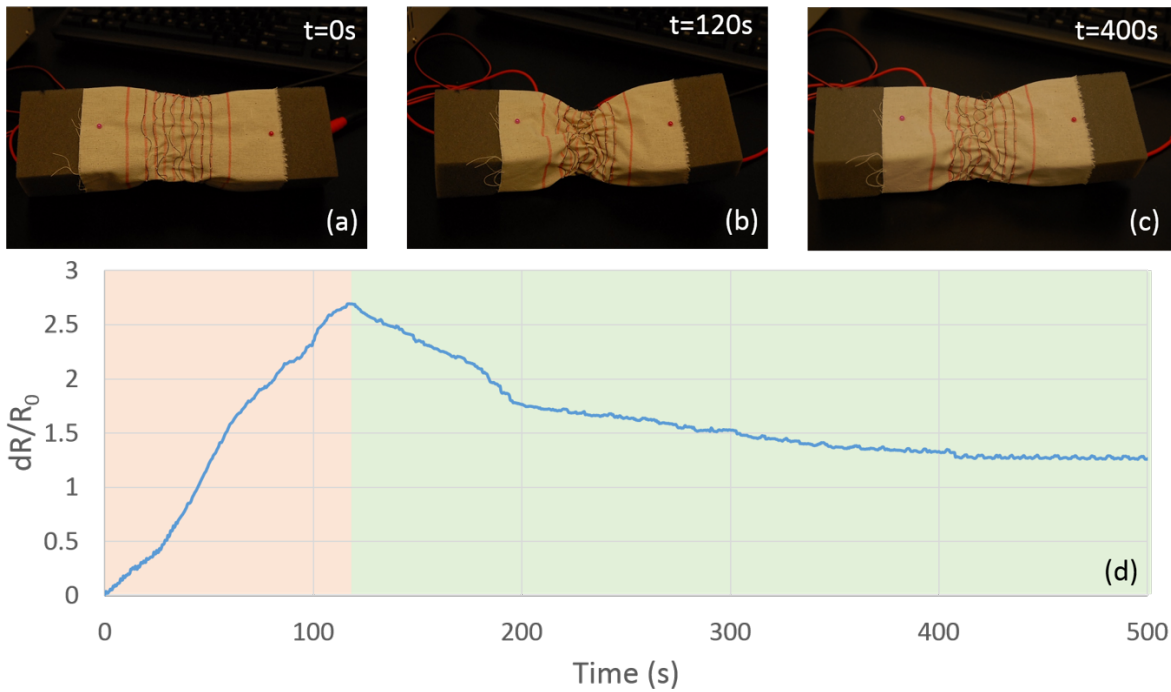


Fig. 9: (a)-(c) Photos of a compression application showing the initial uncompressed state, the maximum compression achieved, and the final semi-decompressed state. (d) Sensor output during compression of a foam block. The red and green shading indicate powered and unpowered SMA, respectively.

responses provide qualitative proprioceptive feedback. In the bending application, the robotic fabric was placed on the inside of the joint to cause flexion. As a result, the sensor decreased in resistance as the joint was flexed because the sensor was less strained (Figure 7). A set of two sensors can thus be used, at a minimum, to qualitatively differentiate between directions of flexion of a joint. Conversely, in the compression application, the robotic fabric was wrapped around a foam block and the sensor increased in resistance as the foam was compressed (Figure 9). In both applications, the robotic fabric contracted, whereas the sensor responses were opposite. Bending and compression can be clearly differentiated and qualitatively correlated with the sensor output.

## VII. FUTURE WORK

The active and sensing thread components of the robotic fabric can be readily integrated using existing textiles technology and methods. In this work, both SMA wire actuators and elastomeric sensors were sewn into the fabric by either hand-sewing or use of a sewing machine. In the future, these components may also be woven into a fabric.

Investigating the interaction between the SMA wire and the fabric, as well as the choice of textile and thread could improve the performance of the actuation unit as a whole. Also, the programming of the SMA can be optimized to improve shape fixity. Control and powering of the SMA can be more precisely regulated to reduce damage to the crystalline structure of the austenite phase and reduce degradation of the shape memory effect.

Introducing multiple sensor threads into a robotic fabric would yield richer sensory information. Not only would the resolution of the sensory output increase, values such as the curvature of the host body could be determined. By combining knowledge of the host body and differential curvature sensing techniques, the overall curvature of the body can be found. Furthermore, the manufacturing methods currently used can be improved towards goals of increased repeatability and robustness. More specifically, more robust sealing methods and elimination of air bubbles in the elastomer tubing used for the sensors should be pursued.

In terms of wearability of the robotic fabric, safety concerns will have to be studied. Because the transition temperature of the SMA wire used here is  $70^{\circ}\text{C}$ , continuous powering of SMA may generate enough thermal energy to burn the skin during sustained direct contact, depending on the duration of contact and the temperature of the contacting object. The threshold temperature for causing minor acute skin burns after 30s exposure is  $48.4^{\circ}\text{C}$  [29]; currently, the maximal temperature on back of the robotic fabric will reach  $50^{\circ}\text{C}$  as measured by a thermocouple (Fluke 87V temperature probe) after a 30s actuation period at 10V and 1.2A. Implementing conservative powering sequences, adding layers of thermal insulation and introducing other thermal management mechanisms will minimize the skin contact temperature.

## VIII. CONCLUSION

In this paper, we have demonstrated how a single sheet of robotic fabric can be used to generate multiple motion

and sensing functions depending on how it is applied to a host body. In particular, we demonstrated that compression and bending motion can be achieved. These two modes of motion are representative of basic motions for a range of robotic applications ranging from wearable robots to new soft industrial robots to autonomous soft robots.

We discussed the fabrication methods and characterization of the actuation and sensing components of robotic fabric. The SMA wire actuator was programmed into a helical coil, then unwound and sewn onto a muslin base fabric in a serpentine pattern. Although increasing the number of returns of SMA on the fabric could increase the contractile force, interactions between the base fabric, stitch thread, and SMA will also play a role in the resulting force production.

The sensor threads are composed of eGaIn-filled silicone tubing. Due to inconsistencies in manufacturing, the response of the sensors are currently non-uniform across different samples. As a result, each thread is currently characterized individually. However, the sensors can reliably qualitatively differentiate between the compressive and bending motions demonstrated by yielding increased and decreased  $dR/R_0$ , respectively.

The integration of actuator threads and sensor threads into a robotic fabric was also demonstrated, and future integration could include higher numbers of each thread. Having a single robotic fabric with actuators and sensors integrated throughout would provide general purpose functionality, and enable new programmable fabrics.

Overall, the introduction of robotic fabrics is expected to contribute towards new exciting possibilities for highly wearable and conformable robots, as well as general soft robots.

## REFERENCES

- [1] S. Kim, E. Hawkes, K. Choy, M. Joldaz, J. Foley, and R. Wood, "Micro artificial muscle fiber using niti spring for soft robotics," in *Intelligent Robots and Systems, 2009. IROS 2009. IEEE/RSJ International Conference on*. IEEE, 2009, pp. 2228–2234.
- [2] E. R. Post and M. Orth, "Smart fabric, or," in *Wearable Computers, 1997. Digest of Papers., First International Symposium on*. IEEE, 1997, pp. 167–168.
- [3] J. Farrington, A. J. Moore, N. Tilbury, J. Church, and P. D. Biemond, "Wearable sensor badge and sensor jacket for context awareness," in *Wearable Computers, 1999. Digest of Papers. The Third International Symposium on*. IEEE, 1999, pp. 107–113.
- [4] D. Bowman and B. Mattes, "Conductive fibre prepared from ultra-high molecular weight polyaniline for smart fabric and interactive textile applications," *Synthetic metals*, vol. 154, no. 1-3, pp. 29–32, 2005.
- [5] A. Lymberis and R. Paradiso, "Smart fabrics and interactive textile enabling wearable personal applications: R&d state of the art and future challenges," in *Engineering in Medicine and Biology Society, 2008. EMBS 2008. 30th Annual International Conference of the IEEE*. IEEE, 2008, pp. 5270–5273.
- [6] M. Pacelli, G. Loriga, N. Taccini, and R. Paradiso, "Sensing fabrics for monitoring physiological and biomechanical variables: E-textile solutions," in *Medical Devices and Biosensors, 2006. 3rd IEEE/EMBS International Summer School on*. IEEE, 2006, pp. 1–4.
- [7] D. Marculescu, R. Marculescu, N. H. Zamora, P. Stanley-Marbell, P. K. Khosla, S. Park, S. Jayaraman, S. Jung, C. Lauterbach, W. Weber *et al.*, "Electronic textiles: A platform for pervasive computing," *Proceedings of the IEEE*, vol. 91, no. 12, pp. 1995–2018, 2003.
- [8] M. A. El-Sherif, J. Yuan, and A. Macdiarmid, "Fiber optic sensors and smart fabrics," *Journal of intelligent material systems and structures*, vol. 11, no. 5, pp. 407–414, 2000.
- [9] A. Grillet, D. Kinet, J. Witt, M. Schukar, K. Krebber, F. Pirotte, and A. Depré, "Optical fiber sensors embedded into medical textiles for healthcare monitoring," *Sensors Journal, IEEE*, vol. 8, no. 7, pp. 1215–1222, 2008.
- [10] M. Pacelli, L. Caldani, and R. Paradiso, "Textile piezoresistive sensors for biomechanical variables monitoring," in *Engineering in Medicine and Biology Society, 2006. EMBS'06. 28th Annual International Conference of the IEEE*. IEEE, 2006, pp. 5358–5361.
- [11] M. Hamedi, L. Herlogsson, X. Crispin, R. Marcilla, M. Berggren, and O. Inganäs, "Fiber-embedded electrolyte-gated field-effect transistors for e-textiles," *Advanced Materials*, vol. 21, no. 5, pp. 573–577, 2009.
- [12] J. B. Lee and V. Subramanian, "Organic transistors on fiber: a first step towards electronic textiles," in *Electron Devices Meeting, 2003. IEDM'03 Technical Digest. IEEE International*. IEEE, 2003, pp. 8–3.
- [13] R. Liu, S. Wang, and T. T. Lao, "A novel solution of monitoring incontinence status by conductive yarn and advanced seamless knitting techniques," *Journal of Engineered Fabrics & Fibers (JEFF)*, vol. 7, no. 4, 2012.
- [14] A. Drimus, G. Kootstra, A. Bilberg, and D. Kragic, "Classification of rigid and deformable objects using a novel tactile sensor," in *Advanced Robotics (ICAR), 2011 15th International Conference on*. IEEE, 2011, pp. 427–434.
- [15] T. Kannaian, R. Neelaveni, and G. Thilagavathi, "Development and characterisation of elastomeric tape sensor fabrics for elbow angle measurement," *Indian Journal of Fibre and Textile Research*, vol. 36, no. 4, p. 436, 2011.
- [16] T. Kaufmann and C. Fumeaux, "Wearable textile half-mode substrate-integrated cavity antenna using embroidered vias," *Antennas and Wireless Propagation Letters, IEEE*, vol. 12, pp. 805–808, 2013.
- [17] J. B. Lee and V. Subramanian, "Weave patterned organic transistors on fiber for e-textiles," *Electron Devices, IEEE Transactions on*, vol. 52, no. 2, pp. 269–275, 2005.
- [18] E. Bonderover and S. Wagner, "A woven inverter circuit for e-textile applications," *Electron Device Letters, IEEE*, vol. 25, no. 5, pp. 295–297, 2004.
- [19] S.-I. Vasile, K. E. Grabowska, I. L. Ciesielska-Wrobel, and J. Ghitaiga, "Analysis of hybrid woven fabrics with shape memory alloys wires embedded," *FIBRES & TEXTILES IN EASTERN EUROPE*, 2010.
- [20] R. Paradiso, A. Gemignani, E. Scilingo, and D. De Rossi, "Knitted bioclothes for cardiopulmonary monitoring," in *Engineering in Medicine and Biology Society, 2003. Proceedings of the 25th Annual International Conference of the IEEE*, vol. 4. IEEE, 2003, pp. 3720–3723.
- [21] Y.-L. Park, B.-r. Chen, D. Young, L. Stirling, R. J. Wood, E. Goldfield, and R. Nagpal, "Bio-inspired active soft orthotic device for ankle foot pathologies," in *Intelligent Robots and Systems (IROS), 2011 IEEE/RSJ International Conference on*. IEEE, 2011, pp. 4488–4495.
- [22] M. Wehner, B. Quinlivan, P. M. Aubin, E. Martinez-Villalpando, M. Bauman, L. Stirling, K. Holt, R. Wood, and C. Walsh, "Design and evaluation of a lightweight soft exosuit for gait assistance," in *2013 IEEE International Conference on Robotics and Automation (ICRA)*, 2013, pp. 6–10.
- [23] S. Seok, C. D. Onal, R. Wood, D. Rus, and S. Kim, "Peristaltic locomotion with antagonistic actuators in soft robotics," in *Robotics and Automation (ICRA), 2010 IEEE International Conference on*. IEEE, 2010, pp. 1228–1233.
- [24] Y. Park, F. Majidi, R. Kramer, P. Bérard, and R. Wood, "Hypere-lastic pressure sensing with a liquid-embedded elastomer," *Journal of Micromechanics and Microengineering*, vol. 20, p. 125029, 2010.
- [25] R. Kramer, C. Majidi, and R. Wood, "Wearable tactile keypad with stretchable artificial skin," in *Robotics and Automation (ICRA), 2011 IEEE International Conference on*. IEEE, 2011, pp. 1103–1107.
- [26] G. Mennitto and M. Buehler, "CARL: a compliant articulated robot leg for dynamic locomotion," *Robotics and autonomous systems*, 1996.
- [27] L. Roos, F. Guenter, A. Guignard, and A. G. Billard, "Design of a biomimetic spine for the humanoid robot robota," in *Biomedical Robotics and Biomechanics, 2006*. IEEE, 2006, p. 329334.
- [28] I. Mizuuchi, R. Tajima, T. Yoshikai, D. Sato, K. Nagashima, M. Inaba, Y. Kuniyoshi, and H. Inoue, "The design and control of the flexible spine of a fully tendon-driven humanoid," in *Intelligent Robots and Systems, 2002. IEEE/RSJ*, vol. 3. IEEE, 2002, p. 25272532.
- [29] P. S. Yarmolenko, E. J. Moon, C. Landon, A. Manzoor, D. W. Hochman, B. L. Viglianti, and M. W. Dewhirst, "Thresholds for thermal damage to normal tissues: An update," *Int J Hyperthermia*, vol. 27, no. 4, pp. 320–343, 2011.